

## Deexcitation $\gamma$ rays following the photodisintegration of $^{17}\text{O}$

G. V. O'Rielly, D. Zubanov,\* and M. N. Thompson

*School of Physics, University of Melbourne, Parkville, Victoria 3052, Australia*

(Received 27 January 1989)

Bremsstrahlung-weighted integrated cross sections for photoproton and photoneutron emission from  $^{17}\text{O}$  to excited residual states in  $^{16}\text{N}$  and  $^{16}\text{O}$  have been measured by detecting the deexcitation  $\gamma$  rays emitted from these states in the residual nuclei. The results are compared with the previously reported  $^{17}\text{O}(\gamma,p)$  and  $^{17}\text{O}(\gamma,n)$  cross sections. About 90% of photoproton emission from  $^{17}\text{O}$  populates the ground-state ( $2^-$ ) and the 0.298-MeV ( $3^-$ ) level in  $^{16}\text{N}$ . It is concluded that this is the result of a single-particle excitation and emission process. The remaining photoproton emission, leading to the 0.120-MeV ( $0^-$ ) and 0.397-MeV ( $1^-$ ) levels, occurs during the preequilibrium stage or from the compound nucleus. The results further indicate that these decay fractions are approximately independent of excitation energy in  $^{17}\text{O}$ . For the  $^{17}\text{O}(\gamma,n)^{16}\text{O}$  reaction, the results show that emission to bound states in  $^{16}\text{O}$  is predominantly to the  $^{16}\text{O}$  ground state ( $0^+$ ), with 4% of the decay from the  $^{17}\text{O}$  giant dipole resonance going to the 6.13-MeV ( $3^-$ ) excited state; population of other bound states is not observed.

### I. INTRODUCTION

The study of the relative population of the residual states formed following photodisintegration of light nuclei can provide information not only about the nature of the dipole states of the excited nucleus, but also about the reaction mechanism. Such studies can be made by detecting the deexcitation  $\gamma$  rays from the residual states, which gives a measure of their relative population. Comparison of these measurements with the spectroscopic factors for the population of the same states following single-nucleon transfer reactions makes it possible to infer the nature of the reaction mechanism. The partial cross sections derived in this way complement investigations of the dipole states through measurement of the total photonuclear-reaction cross sections.

This paper reports measurements of the integrated cross sections for population of residual states following photonuclear reactions in  $^{17}\text{O}$ . This complements measurements of the  $^{17}\text{O}$  photoneutron cross section,<sup>1</sup> and the  $^{17}\text{O}$  photoproton cross section.<sup>2</sup> For the  $^{17}\text{O}(\gamma,p)^{16}\text{N}$  reaction, measurements of the deexcitation spectra were made at four bremsstrahlung energies, extending from just above the reaction threshold to beyond the giant dipole resonance (GDR). This allowed the relative population of residual states to be determined as a function of excitation in  $^{17}\text{O}$ . In the case of the  $^{17}\text{O}(\gamma,n)^{16}\text{O}$  reaction, a separate measurement was made at a single bremsstrahlung energy of 28 MeV, thus providing only a measure of the integrated cross section from all dipole states in  $^{17}\text{O}$  up to this energy.

### II. EXPERIMENTAL DETAILS

A 120-g sample of water, isotopically enriched to 48.6% in  $^{17}\text{O}$ , was contained in a thin-walled Lucite cylinder 3.81 cm in diameter, and 10.2 cm long. This sample was irradiated in the bremsstrahlung beam from

the 35-MeV betatron at the University of Melbourne. The beam was collimated to a spot 3.5 cm in diameter at the sample position. The photon flux was monitored using a thin-walled transmission ionization chamber, which was intercalibrated against a replica standard NBS-P2 chamber.<sup>3</sup> Two separate experiments were performed, the first to measure the deexcitation  $\gamma$  rays associated with the  $^{17}\text{O}(\gamma,p)^{16}\text{N}$  reaction, and the second to measure those from the  $^{17}\text{O}$  photoneutron reaction.

#### A. Deexcitation $\gamma$ rays following photoproton emission from $^{17}\text{O}$

Photoproton emission from  $^{17}\text{O}$  to bound states of  $^{16}\text{N}$  can populate only the four lowest states; the ground state or the states at 120, 298, and 397 keV, as shown in Fig. 1. Although the experimental techniques for observing prompt deexcitation  $\gamma$  rays are well established and documented,<sup>4-6</sup> particular problems exist when  $\gamma$  rays with energies as low as those in this experiment are involved. The intense flux of scattered photons due to Compton and other atomic processes produced by the bremsstrahlung beam in the sample makes detection of such low-energy deexcitation  $\gamma$  rays impossible. Fortunately the first excited state of  $^{16}\text{N}$ , at 120 keV, has a half-life of 5.25  $\mu\text{s}$ ,<sup>7</sup> which is sufficiently long to enable the detection of the deexcitation  $\gamma$  rays from this level after the 3- $\mu\text{s}$ -long bremsstrahlung beam from the betatron. Deexcitation  $\gamma$  rays may be emitted from the 120-keV state either following its population directly by photoproton emission from  $^{17}\text{O}$ , or following a (73%) prompt  $\gamma$  branch from the 397-keV state. These 120-keV  $\gamma$  rays were detected using a thin Ge(Li) low-energy photon detector, with the data-acquisition system enabled to count for 70  $\mu\text{s}$  starting 8.5  $\mu\text{s}$  after the beam burst.

Although data were recorded only outside the bremsstrahlung beam burst, it was still necessary to protect the detector from the relatively intense scattered beam. This

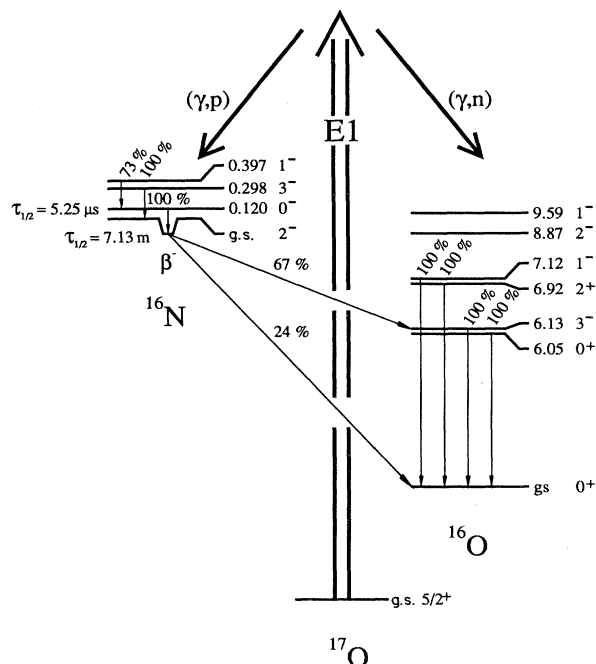


FIG. 1. Relevant level and decay data from Ref. 7 for the photonuclear reactions on  $^{17}\text{O}$ .

was achieved in several ways. Firstly the detector was surrounded with 15 cm of lead, except for an opening towards the  $^{17}\text{O}$  sample, and was placed at as large an angle relative to the beam as was physically possible ( $138^\circ$ ) in order to minimize the intensity of the Compton-scattered radiation. In addition, the bremsstrahlung beam was hardened by placing  $58 \text{ g/cm}^2$  of graphite in the beam between the bremsstrahlung radiator and the shielding wall. Despite these measures, the detector took about  $100 \mu\text{s}$  to recover completely from the saturation effects produced by the beam burst. During this period the detector had a dead time that depended on the time after the beam burst. This reduction in detection efficiency was quantified as a function of time after the beam burst by measuring, under normal experimental conditions, the count rate of 122-keV  $\gamma$  rays from a  $^{57}\text{Co}$  source placed near the sample. The efficiency curve obtained was modified to allow for the  $5.25\text{-}\mu\text{s}$  half-life of the  $^{16}\text{N}^*$   $0.120\text{-MeV}$  ( $0^-$ ) level in order to determine the effective gating factor. The absolute detector efficiency for 120-keV  $\gamma$  rays was determined using a calibrated  $^{57}\text{Co}$  source placed at various positions along the location of the sample axis, with the bremsstrahlung beam off and the detectors in the experimental geometry.

In order to determine the fraction of photoproton decays which populate the 120-keV level in  $^{16}\text{N}$ , a measure of the bremsstrahlung-weighted integrated cross section for the total photoproton reaction is required. This measurement was made concurrently with that of the deexcitation  $\gamma$  rays from the 120-keV level in  $^{16}\text{N}$ , and when compared with the bremsstrahlung-weighted cross section derived from the work of Zubanov *et al.*,<sup>2</sup> allowed a check on the reliability of the present experimental and

data reduction techniques.

The  $^{17}\text{O}(\gamma,p)^{16}\text{N}$  reaction is identified by the 7.13-s half-life  $\beta^-$  decay of the residual  $^{16}\text{N}$  nucleus. The  $\beta^-$  decay of  $^{16}\text{N}$  is predominantly (67%) (Ref. 7) to the second excited state of  $^{16}\text{O}$ , which decays promptly, emitting a 6.13-MeV  $\gamma$  ray (see Fig. 1). Measurement of the 6.13-MeV  $\gamma$  rays observed outside the beam burst allows the bremsstrahlung-weighted integrated cross section for this reaction to be determined. These signature  $\gamma$  rays were detected using a well-shielded  $45 \text{ cm}^3$  intrinsic-germanium detector positioned close to the sample at an angle of  $90^\circ$  to the incident beam direction. The counting system was gated so that 6.13-MeV  $\gamma$  rays were emitted between beam bursts, and more than 1 ms after the beam bursts were recorded, thus providing a gating efficiency of 95%. The absolute efficiency of the detector for 6.13-MeV  $\gamma$  rays was determined using a calibrated  $\text{Cm-}^{13}\text{C}$  source, which produces 6.13-MeV  $\gamma$  rays via the  $^{13}\text{C}(\alpha,n)^{16}\text{O}$  reaction.

Gamma-ray spectra were recorded for bremsstrahlung end-point energies of 16.5, 18.5, 21.5, and 28.0 MeV. These energies were chosen to cover the energy region of the reported  $^{17}\text{O}(\gamma,p)^{16}\text{N}$  cross section.<sup>2</sup> In particular, the measurement at 28.0 MeV was used to determine the relative population of residual states for proton decay integrated beyond the GDR region of  $^{17}\text{O}$ . The other energies were selected to study proton emission from the structure below the GDR, with emphasis on the pronounced resonance reported at 15.1 MeV.

Figure 2 shows the raw spectra collected using the low-energy photon detector. Data collection times were in excess of 24 h at each bremsstrahlung energy, and in-

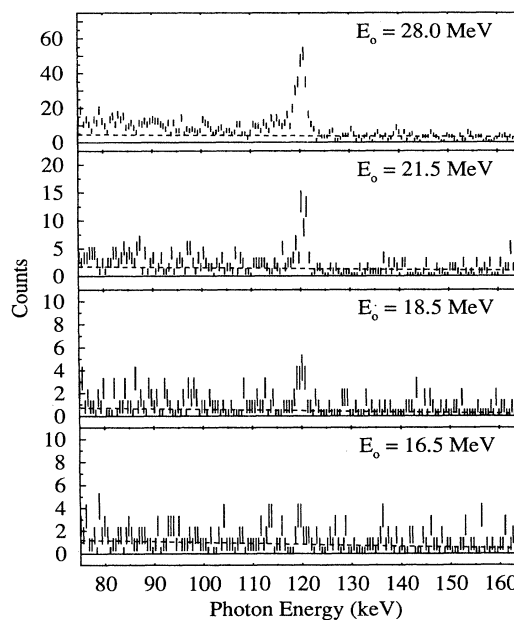


FIG. 2. Spectra recorded at four bremsstrahlung end-point energies indicating decay of the 120-keV level in  $^{16}\text{N}$  following the  $^{17}\text{O}(\gamma,p)$  reaction. The dashed line indicates the background determined as described in the text.

creased to 48 h for the 16.5-MeV point. The poor statistics can be directly attributed to the low detector efficiency and the low photon flux available from the betatron.

### B. Deexcitation $\gamma$ rays following photon-neutron emission from $^{17}\text{O}$

The bremsstrahlung-weighted integrated cross sections for the population of states in  $^{16}\text{O}$  following the  $^{17}\text{O}(\gamma, n)$  reaction were measured in a separate experiment. In this case, because the relevant deexcitation  $\gamma$  rays have energies greater than 6 MeV (see Fig. 1), it was possible to detect these prompt  $\gamma$  rays during the beam burst. The problem of photons scattered from the sample that precluded this procedure for the low-energy  $\gamma$  rays from  $^{16}\text{N}$ , following the  $^{17}\text{O}(\gamma, p)$  reaction, was much reduced in this measurement. The deexcitation  $\gamma$  rays were detected using a well-shielded intrinsic-germanium detector. In order to reduce pile-up and dead-time effects resulting from the intense scattered beam, the detector was placed at a backward angle of  $135^\circ$ , and the bremsstrahlung beam was hardened, as described for the  $^{17}\text{O}(\gamma, p)^{16}\text{N}$  measurement. The detector was housed in a 15-cm-thick shield of lead, and a 1-cm-thick filter of lead was placed over the opening in this shielding. The effects of scattering from the sample were further reduced by lengthening the contraction time of the electron beam onto the bremsstrahlung radiator of the betatron, to provide a 380- $\mu\text{s}$ -long beam burst. Since the  $\gamma$  rays of interest are prompt deexcitations, the data-acquisition system was gated so that only events produced during the beam were recorded. The measurement was made at a single end-point energy of 28 MeV.

### III. ANALYSIS

The number of deexcitation  $\gamma$  rays detected at a particular bremsstrahlung end-point energy reflects the differential cross section over the energy region up to this end-point energy weighted by the number of photons at each energy in the hardened bremsstrahlung spectrum. This “bremsstrahlung-weighted” integrated cross section is defined as

$$\frac{d\sigma_{\text{BW}}}{d\Omega} = \int_0^{E_0} N(E_0, E) \frac{d\sigma(E)}{d\Omega} dE = Y(E_0)F(E_0)A,$$

where  $N(E_0, E)$  is the hardened bremsstrahlung number

spectrum at end-point energy  $E_0$ ,  $d\sigma(E)/d\Omega$  is the cross section for population of the specific state,  $Y(E_0)$  is the experimental yield at end-point energy  $E_0$ ,  $F(E_0)$  normalizes the bremsstrahlung spectrum to unit dose, and  $A$  contains the detector and sample factors. The analysis of the data from deexcitation  $\gamma$ -rays experiments generally yields differential cross sections, with an angular distribution given by<sup>6</sup>

$$\frac{d\sigma_{\text{BW}}(\theta)}{d\Omega} = \frac{\sigma_{\text{BW}}}{4\pi} [1 + aP_2(\cos\theta)],$$

where  $d\sigma_{\text{BW}}(\theta)/d\Omega$  is the differential cross section at angle  $\theta$ ,  $\sigma_{\text{BW}}$  is the “bremsstrahlung-weighted” cross section, and  $a$  is a constant.

For  $\theta=135^\circ$ , the angle at which deexcitation  $\gamma$  rays were detected in the present measurement,  $P_2(\cos\theta)$  is small (0.25) [ $P_2(\cos\theta)$  has a zero at  $125^\circ$ ] so that for values of  $a$  in the expected range 0.25–0.45,<sup>8</sup> the total “bremsstrahlung-weighted” integrated cross section can be approximated to within 10% by  $4\pi[d\sigma(\theta)/d\Omega]$ . No such approximation was made in the analysis of the data from the photoproton measurement, as an isotropic angular distribution can be assumed for the 120-keV and the 6.13-MeV deexcitation  $\gamma$  rays since the parent states involved are long lived.

### A. Integrated cross sections for the $^{17}\text{O}(\gamma, p)^{16}\text{N}$ reaction to excited states

The “bremsstrahlung-weighted” integrated cross section for the population of the 0.120-MeV ( $0^-$ ) level was determined from the number of 120-keV events in the spectrum recorded at a given bremsstrahlung energy. This number was the sum of the counts in the spectrum over the energy region from 95 to 125 keV. Because this integration region included both the photoelectric peak and part of the Compton response of the detector, it was important to check that this region included only events associated with the 120-keV  $\gamma$  ray of interest. An experimental detector response, determined using 122-keV  $\gamma$  rays from a  $^{57}\text{Co}$  source, was compared with the experimental spectrum. The agreement was excellent in the energy region used in the cross-section calculation. The background was assumed to be linear in and near the region used in the analysis. It was determined by making a linear fit to the counts in the spectrum immediately above the photopeak (from 130 to 160 keV). This fit was extra-

TABLE I. The “bremsstrahlung-weighted” integrated cross sections quoted have been normalized such that the hardened bremsstrahlung spectrum contains a single photon. The uncertainties quoted with each value are statistical only, with the systematic errors determined by a linear sum of the contributing uncertainties.

	Value (MeV mb $\times 10^{-2}$ )	End-point energy, $E_0$				Systematic error
		16.5 MeV	18.5 MeV	21.5 MeV	28.0 MeV	
$(\gamma, p_{\text{tot}})$	Present work	3.1 $\pm$ 0.6	5.4 $\pm$ 0.5	10.9 $\pm$ 0.6	37 $\pm$ 3	$\pm$ 17%
	Ref. 2	3.80 $\pm$ 0.07	6.42 $\pm$ 0.09	12.1 $\pm$ 0.1	34.9 $\pm$ 0.1	$\pm$ 10%
$(\gamma, p_{1,3})$	Present work	0.29 $\pm$ 0.14	0.76 $\pm$ 0.24	0.94 $\pm$ 0.17	3.93 $\pm$ 0.33	$\pm$ 8%

polated into the region of interest.

The spectra that were taken simultaneously, using the intrinsic-germanium detector, showed the 6.13- and 7.12-MeV  $\gamma$  rays from  $^{16}\text{O}$  following the  $\beta^-$  decay of  $^{16}\text{N}$ . The sum of the areas of the full-energy, single-escape and the double-escape peaks of the 6.13-MeV  $\gamma$  rays were used to determine the "bremsstrahlung-weighted" integrated cross section for the  $^{17}\text{O}(\gamma,p)^{16}\text{N}$  reaction. In determining the efficiency of the detector for these  $\gamma$  rays using the spectrum from the Cm- $^{13}\text{C}$  source, the same integration regions were used.

The integrated counts for both the 120-keV and 6.13-MeV spectra were corrected for the detector efficiencies, branching ratios, and the gating factors. The correction for  $\gamma$ -ray absorption in the sample was determined for both the 120-keV and 6.13-MeV  $\gamma$  rays using a Monte Carlo simulation. "Bremsstrahlung-weighted" integrated cross sections were calculated at each end-point energy for photoproton emission to the  $(0^-)$  and  $(1^-)$  levels in  $^{16}\text{N}$  and for the  $^{17}\text{O}(\gamma,p_{\text{total}})^{16}\text{N}$  reaction, and are listed in Table I. As a comparison, the "bremsstrahlung-weighted" integrated cross sections at the same energies were calculated from the reported  $^{17}\text{O}(\gamma,p_{\text{total}})^{16}\text{N}$  cross section,<sup>2</sup> by convoluting the total cross section with a photon spectrum derived from the Schiff integrated-over-angles bremsstrahlung spectrum<sup>9</sup> after correcting for the effect of the beam hardener on the spectrum. The results of this calculation are also listed in Table I. The agreement between the values of the "bremsstrahlung-weighted" integrated  $^{17}\text{O}(\gamma,p)^{16}\text{N}$  cross section reported here, with those deduced from Ref. 2, is reasonable, and validates the method and analysis presented here.

On the basis of a simple assumption it is possible to extract values for the integrated (non-bremsstrahlung-weighted) cross sections from the above-mentioned data. If it is assumed that the partial and total  $^{17}\text{O}(\gamma,p)^{16}\text{N}$  cross sections have the same shape, then the ratio of the "bremsstrahlung-weighted" integrated total cross section to the integrated total cross section determined from Ref. 2, allows the integrated partial cross sections to be deduced from the present measurement of the "bremsstrahlung-weighted" integrated partial cross sections. It is estimated that the assumption of similar shapes introduces a systematic uncertainty of about 5%.

The partial cross section, integrated up to the various end-point energies, for proton decay from  $^{17}\text{O}$  leading to emission of a  $\gamma$ -ray from the 120-keV state, and for the  $^{17}\text{O}(\gamma,p)^{16}\text{N}$  reaction, are listed in Table II. The results clearly show that only a small fraction of the total integrated cross section of the  $^{17}\text{O}(\gamma,p)^{16}\text{N}$  reaction leads to emission of a  $\gamma$  ray from the 120-keV state. Since this level can be populated either directly by proton emission from  $^{17}\text{O}$  or by  $\gamma$  decay from the 397-keV level (73% branching) following its population via proton decay from  $^{17}\text{O}$ , the conclusion from the data is limited to a statement that only a small fraction ( $11\pm 4\%$ ) of photoproton decay leads to population of either or both of the 120- or 397-keV levels in  $^{16}\text{N}$ . The major decay mode (about 90%) is to the ground state or the 298-keV state.

#### B. Integrated cross section for the $^{17}\text{O}(\gamma,n)^{16}\text{O}$ reaction to excited states

The integrated cross sections for population of excited states in  $^{16}\text{O}$ , following the  $^{17}\text{O}(\gamma,n)^{16}\text{O}$  reaction, were deduced from the in-beam spectra recorded during the second measurement. The analysis was complicated by the fact that the  $^{17}\text{O}$ -enriched sample contained 24%  $^{16}\text{O}$ , which, following photodisintegration, will populate states in  $^{15}\text{N}$  and  $^{15}\text{O}$ . Deexcitation  $\gamma$  rays from these nuclei complicate the spectrum. In particular, the  $\gamma$  ray from the decay of the 6.323-MeV state in  $^{15}\text{N}$  will partially overlap the deexcitation  $\gamma$  rays from the first two excited states in  $^{16}\text{O}$  (6.052 and 6.131 MeV). The deexcitation  $\gamma$  rays from  $^{15}\text{O}$  and  $^{15}\text{N}$  were measured in a separate experiment done using a natural water sample. The  $\gamma$  ray spectrum obtained was normalized by dose and mass of  $^{16}\text{O}$  to the spectrum obtained using the  $^{17}\text{O}$ -enriched sample, and subtracted from this spectrum. The resulting  $\gamma$ -ray spectrum contained only deexcitation  $\gamma$  rays from residual states populated from the  $^{17}\text{O}(\gamma,n)$  reaction, and showed population of the  $^{16}\text{O}$  6.13-MeV ( $3^-$ ) level only. There was no evidence of population of any of the other bound levels.

The "bremsstrahlung-weighted" integrated cross section for the population of the 6.13-MeV level in  $^{16}\text{O}$  was calculated from the summed counts in the full-energy, single-escape and double-escape spectral peaks. After al-

TABLE II. Integrated photonuclear cross sections for the  $^{17}\text{O}(\gamma,p)$  reaction. The uncertainties quoted with each value are statistical only, with the systematic errors determined by a linear sum of the contributing uncertainties.

	Value (MeV mb)	End-point energy, $E_0$				Systematic error
		16.5 MeV	18.5 MeV	21.5 MeV	28.0 MeV	
$(\gamma,p_{\text{tot}})$	Present work	$1.4\pm 0.3$	$2.4\pm 0.2$	$5.6\pm 0.3$	$21\pm 2$	$\pm 17\%$
	Ref. 2	$1.73\pm 0.03$	$2.84\pm 0.03$	$6.13\pm 0.04$	$20.2\pm 0.1$	$\pm 10\%$
$(\gamma,p_{1,3})$	Present work	$0.13\pm 0.06$	$0.34\pm 0.11$	$0.47\pm 0.09$	$2.3\pm 0.2$	$\pm 13\%$
Fraction of $(\gamma,p)$ decays to $^{16}\text{N}$ 0.120-MeV ( $0^-$ ) level		$7.5\pm 3.5$	$12.0\pm 3.9$	$7.7\pm 1.5$	$11.4\pm 1.0$	$\pm 18\%$

lowance for absorption, detector efficiency, and dose, in a similar way to that already described for the  $^{17}\text{O}(\gamma,p)^{16}\text{N}$  data, a value of  $(0.20 \pm 0.04)$  MeV mb was obtained for the "bremsstrahlung-weighted" cross section integrated up to 28 MeV. This value is to be compared with the "bremsstrahlung-weighted" cross sections integrated up to 28.0 MeV for the total  $^{17}\text{O}(\gamma,n)^{16}\text{N}$  reaction, derived from the measurement by Jury *et al.*,<sup>1</sup> of  $(7.28 \pm 0.01)$  MeV mb and the  $^{17}\text{O}(\gamma,n_0)^{17}\text{O}$ , derived from the data of Jury *et al.*,<sup>10</sup> of  $(2.124 \pm 0.002)$  MeV mb. In each case there is a systematic error of 10% in addition to the errors indicated.

#### IV. DISCUSSION

Although in heavy nuclei the photonuclear reaction mechanism is generally agreed to involve, predominantly, the excitation of collective dipole states which subsequently decay by an evaporative process, the situation for light nuclei is different. In light nuclei there is ample evidence from both deexcitation  $\gamma$  ray studies<sup>11</sup> and studies of photoproton spectra<sup>12</sup> that a direct or semidirect process is involved, and is generally dominant. It is useful to quantify the probability that a nucleon, having been excited to a continuum dipole state (the doorway state) will be directly emitted (the semidirect process), or will undergo successive interactions to form more complex  $n$ -particle  $n$ -hole configurations until a compound nucleus is formed. Nucleon emission from the compound nucleus or earlier, at the preequilibrium stage, gives access to a larger range of residual states, with more complex configurations, than does the semidirect process.<sup>13</sup> The data presented in this paper allow a clarification of the reaction process involved in the case of  $^{17}\text{O}$ .

##### A. Photoproton emission from $^{17}\text{O}$

Consider first the relative population of states in  $^{16}\text{N}$  following the  $^{17}\text{O}(\gamma,p)^{16}\text{N}$  reaction using a shell-model description. The reaction mechanism may be inferred by considering which  $^{16}\text{N}$  states could be formed by emission of a proton from the dipole states of  $^{17}\text{O}$ .

Protons emitted from  $^{17}\text{O}$  to bound states in  $^{16}\text{N}$  may populate the four lowest states, the ground state ( $2^-$ ), or one of a triplet of excited states at 120, 298, and 397 keV; all higher states in  $^{16}\text{N}$  are neutron unstable. The wave functions of these bound states are known to be almost pure 1p-1h in nature. Shell-model calculations<sup>14</sup> using a full  $p$ - $s$ - $d$  shell basis space give, as the dominant (96%) component of the  $^{16}\text{N}$  ground state ( $2^-$ ) and the 0.298-MeV ( $3^-$ ) state, a 1p-1h configuration of the type  $|(p_{1/2})^{-1}(d_{5/2})^1\rangle$ . For the 0.120-MeV ( $0^-$ ) and 0.397-MeV ( $1^-$ ) states, the dominant (> 96%) configuration is  $|(p_{1/2})^{-1}(s_{1/2})^1\rangle$ . Calculations by Brown and Green<sup>15</sup> for  $^{17}\text{O}$  indicate that the ground-state wave function consists predominantly (81%) of a ( $d_{5/2}$ ) neutron outside a closed  $p$ -shell core, with minor (16%) 3p-2h configurations of the type  $|(p_{1/2})^{-2}(d_{5/2})^3\rangle$ .

Population of 1p-1h states in  $^{16}\text{N}$  thus requires the formation of a 2p-1h doorway state in  $^{17}\text{O}$ , through the excitation of a  $p_{1/2}$  nucleon from the major configuration  $|(d_{5/2})^1\rangle$  of the  $^{17}\text{O}$  ground state. If the photoproton re-

action mechanism is regarded as being the  $E1$  excitation of a particular proton, followed by its emission, then this would result in population of those states in  $^{16}\text{N}$  with predominantly  $|(p_{1/2})^{-1}(d_{5/2})^1\rangle$  configurations, i.e., consistent with the  $^{16}\text{N}$  ground state ( $2^-$ ) and the 0.298-MeV ( $3^-$ ) state; but not the 0.120-MeV ( $0^-$ ) or 0.397-MeV ( $1^-$ ) states.

The results of this experiment indicate (see Table II) that approximately 90% of photoproton emission from  $^{17}\text{O}$  populates one or the other of the ground state ( $2^-$ ) or 0.298-MeV ( $3^-$ ) state in  $^{16}\text{N}$ , since only about 10% of the total  $^{17}\text{O}(\gamma,p)^{16}\text{N}$  cross section leads to decay of the 0.120-MeV level in  $^{16}\text{N}$ . These fractions are similar over the energy range from near threshold to above the GDR.

A similarly strong population of these states is observed in the proton pick-up reaction  $^{17}\text{O}(d,^3\text{He})^{16}\text{N}$ .<sup>16</sup> As the pick-up reaction is a direct process, this implies that the population of the  $^{16}\text{N}$  ( $2^-$ ) and ( $3^-$ ) states through the photoproton reaction is via a similarly direct reaction mechanism. Correlations between the relative population of residual states following single-particle photoemission from light nuclei, and the spectroscopic factors for the same states, have been observed in other measurements.<sup>5,12,13,17-19</sup>

While a semidirect description of the photoproton reaction explains the population of the  $^{16}\text{N}$  ( $2^-$ ) and ( $3^-$ ) states, it does not account for the observed 10% population of the 0.120-MeV ( $0^-$ ) and 0.397-MeV ( $1^-$ ) states. As already noted, these states have essentially pure  $|(p_{1/2})^{-1}(s_{1/2})^1\rangle$  configurations, and as such cannot be formed by excitation and emission of a single proton from the  $^{17}\text{O}$  ground state, with its dominant ( $d_{5/2}$ ) particle component. Rather, a significant rearrangement of the nucleons is necessary. That is, population of the  $^{16}\text{N}$  ( $0^-$ ) and ( $1^-$ ) states requires the formation of more complicated states in  $^{17}\text{O}$  than those leading to the population of the ( $2^-$ ) and ( $3^-$ ) states. The absence of population of the ( $0^-$ ) and ( $1^-$ ) states in  $^{16}\text{N}$  following the  $^{17}\text{O}(d,^3\text{He})^{16}\text{N}$  pick-up reaction confirms this conclusion.

In order to determine the fraction of semidirect processes in the photoproton cross section it was assumed that the semidirect process dominated the decay to the residual nucleus ground state. The evidence for this comes from the distinct correlation observed between the spectroscopic factors for the residual nucleus ground state and the population of the ground state in the photoproton reaction, and also from fluctuation analysis of fine structure in the photoproton cross section, for many light nuclei.<sup>13</sup>

Since the  $^{16}\text{N}$  ground state ( $2^-$ ) and 0.298-MeV ( $3^-$ ) states have an essentially identical configuration, it is reasonable to suppose that they are populated via the same reaction mechanism. Further, as the  $^{16}\text{N}^*$  ( $1^-$ ) and ( $0^-$ ) states can only be populated through decay from the preequilibrium or compound-nucleus states, the present results suggest that the  $^{17}\text{O}(\gamma,p)$  reaction is approximately 90% semidirect in nature. Comparison between the spectroscopic factors and the relative population of states in  $^{16}\text{N}$ , together with the wave functions for these states, is shown in Table III.

Eramzhyan *et al.*<sup>13</sup> have reviewed published photopro-

TABLE III. The relative population of states in  $^{16}\text{N}$  via the  $^{17}\text{O}(\gamma, p)^{16}\text{N}$  reaction from this work, and the spectroscopic factors for population of the same states via the pick-up reaction  $^{17}\text{O}(d, ^3\text{He})^{16}\text{N}$  from Ref. 16. The wave functions, from Elliot and Flowers (Ref. 14), are shown for the states of interest.

Level (MeV)	$J^\pi$	Wave function	Relative population ( $\gamma, p$ )	$C^2S$ ( $d, ^3\text{He}$ )
g.s.	$2^-$	96% $ (p_{1/2})^{-1}(d_{5/2})^1\rangle + 2\%  (p_{3/2})^{-1}(d_{5/2})^1\rangle$	~90%	0.94
0.298	$3^-$	96% $ (p_{1/2})^{-1}(d_{5/2})^1\rangle + 3\%  (p_{3/2})^{-1}(d_{5/2})^1\rangle$		1.33
0.120	$0^-$	100% $ (p_{1/2})^{-1}(s_{1/2})^1\rangle$	~10%	
0.397	$1^-$	96% $ (p_{1/2})^{-1}(s_{1/2})^1\rangle + 3\%  (p_{3/2})^{-1}(s_{1/2})^1\rangle$		

ton data on the relative population of residual states, in order to establish the importance of the semidirect process in light nuclei. Their results show that the semidirect component of photoproton decay for *odd-even* nuclei is smaller than for neighboring *even-even* nuclei by a factor between 1.5 and 2. They conclude that the presence of an unpaired nucleon leads to an increase in the probability for the dipole states to decay through a compound-nucleus stage. This conclusion is not borne out for the  $^{17}\text{O}$ ,  $^{16}\text{O}$  pair. Eramzhyan *et al.*<sup>13</sup> give a value of  $(0.83 \pm 0.07)$  for the probability of a semidirect process in the  $^{16}\text{O}(\gamma, p)^{15}\text{N}$  reaction. The data in the present paper suggest that for the  $^{17}\text{O}(\gamma, p)^{16}\text{N}$  reaction, the semidirect component is from 0.85 to 0.93; not significantly different than that for the  $^{16}\text{O}(\gamma, p)$  reaction. However, the conclusions of Eramzhyan *et al.*<sup>13</sup> are probably more valid for nuclei in the  $(2s-1d)$  shell, where the wave functions may have more complex admixtures, with a consequent increase in the probability of compound-nucleus formation. In the case of  $^{16}\text{O}$  and  $^{17}\text{O}$  the  $1p$  shell is closed, reducing the chance of complex admixtures in the wave functions.

### B. Photoneutron emission from $^{17}\text{O}$

Shell-model calculations<sup>15,20</sup> using a  $p$ - $s$ - $d$  basis space have been made for the wave functions of states in  $^{16}\text{O}$ . These show that the major component (76%) of the  $^{16}\text{O}$  ground state is a closed  $p$ -shell core, with some (22%)  $2p$ - $2h$  configurations of the type  $|(p_{1/2})^{-2}(d_{5/2})^2\rangle$ . The

other two bound, positive-parity states, at 6.05 MeV ( $0^+$ ) and 6.92 MeV ( $2^+$ ), have predominately (88% and 85%, respectively)  $4p$ - $4h$  components, with only minor  $0p$ - $0h$  components in their wave functions. The negative parity states below 9 MeV have wave functions with mostly  $1p$ - $1h$  and  $3p$ - $3h$  components.

Using the description of Brown and Green<sup>15</sup> of the  $^{17}\text{O}$  ground-state wave function,  $E1$  excitation will involve either excitation of a  $p_{1/2}$  subshell particle of the  $(2s-1d)$  subshell, giving basic configurations of  $(p_{1/2})^{-1}(2s-1d)^2$  and  $(p_{1/2})^{-3}(2s-1d)^4$ , or excitation from the  $(d_{5/2})$  subshell to the  $(2p-1f)$  shell. The excitation and subsequent emission of a  $d_{5/2}$  neutron from the ground state of  $^{17}\text{O}$  will result in population of residual states in  $^{16}\text{O}$  with configurations consistent with the  $^{16}\text{O}$  ground state. The excitation and emission of a  $p_{1/2}$ -subshell neutron from  $^{17}\text{O}$  ground state will give access to residual states with wave functions having  $|(p_{1/2})^{-1}(d_{5/2})^1\rangle$  as their leading component, with minor  $|(p_{1/2})^{-3}(d_{5/2})^3\rangle$  components. This description is consistent with the 6.13-MeV ( $3^-$ ) and 8.87-MeV ( $2^-$ ) levels in  $^{16}\text{O}$ . The positive-parity states in  $^{16}\text{O}$ , at 6.05 MeV ( $0^+$ ) and 6.92 MeV ( $2^+$ ), are predominantly  $4p$ - $4h$  in nature, and are not expected to be populated via a single-particle excitation and emission process. Similarly, the 7.12-MeV ( $1^-$ ) level, with occupation of the  $s_{1/2}$  subshell, will not be populated via such a semidirect process.

The results of this experiment indicate that the only bound excited state in  $^{16}\text{O}$  populated following the  $^{17}\text{O}(\gamma, n)$  reaction is that at 6.13 MeV ( $3^-$ ). The failure

TABLE IV. The relative population of states in  $^{16}\text{O}$  via  $^{17}\text{O}(\gamma, n)^{16}\text{O}$  reaction from this work, and the spectroscopic factors for population of the same states via the pick-up reaction  $^{17}\text{O}(d, ^3\text{H})^{16}\text{O}$  from Ref. 16. The wave functions, from Zuker *et al.* (Ref. 20), are shown for the states of interest.

Level (MeV)	$J^\pi$	Wave function	Relative population ( $\gamma, n$ )	$C^2S$ ( $d, ^3\text{H}$ )
6.05	$0^+$	11% $0p$ - $0h$ + 38% $ (p_{1/2})^{-4}(s_{1/2})^4\rangle +$ 31% $ (p_{1/2})^{-4}(d_{5/2})^2(s_{1/2})^2\rangle$	<0.1%	
6.13	$3^-$	66% $ (p_{1/2})^{-1}(d_{5/2})^1\rangle + 25\%  (p_{1/2})^{-3}(d_{5/2})^3\rangle$	$(3.9 \pm 0.8)\%$	0.46
6.92	$2^+$	14% $ (p_{1/2})^{-2}(d_{5/2})^2\rangle + 15\%  (p_{1/2})^{-2}(d_{5/2})^1(s_{1/2})^1\rangle +$ 12% $ (p_{1/2})^{-4}(d_{5/2})^4\rangle + 18\%  (p_{1/2})^{-4}(d_{5/2})^1(s_{1/2})^3\rangle +$ 22% $ (p_{1/2})^{-4}(d_{5/2})^2(s_{1/2})^2\rangle$		
7.12	$1^-$	48% $ (p_{1/2})^{-1}(s_{1/2})^1\rangle + 13\%  (p_{1/2})^{-3}(s_{1/2})^3\rangle +$ 29% $ (p_{1/2})^{-3}(d_{5/2})^2(s_{1/2})^1\rangle$	<0.1%	
8.89	$2^-$	66% $ (p_{1/2})^{-1}(d_{5/2})^1\rangle + 22\%  (p_{1/2})^{-3}(d_{5/2})^3\rangle$	$\alpha$ unstable	0.33

to observe deexcitation gamma rays from the other levels (6.05, 6.92, and 7.12 MeV) indicates that the relative population of these is less than 0.1%. Deexcitation  $\gamma$  rays will not be observed from the 8.89-MeV ( $2^-$ ) level as it decays by  $\alpha$  emission directly to the  $^{12}\text{C}$  ground state. Although this experiment cannot deduce the population of the  $^{16}\text{O}$  ground state, this information is available from the measurement of the  $^{17}\text{O}(\gamma, n_0)^{16}\text{O}$  cross section.<sup>10</sup>

The  $^{16}\text{O}$  ground state ( $0^+$ ) and 6.13-MeV ( $3^-$ ) levels are strongly populated in the neutron pick-up reaction  $^{17}\text{O}(d, t)^{16}\text{O}$  (Ref. 16) via  $d_{5/2}$  and  $p_{1/2}$  neutron pick up, respectively. The population of the  $^{16}\text{O}$  ground state dominates the  $l=2$  ( $d_{5/2}$ ) neutron pick up, with the population of higher levels being almost entirely due to pick up from the  $p$  shell. With the  $^{17}\text{O}$  photoneutron reaction it is understood<sup>10</sup> that the  $^{17}\text{O}(\gamma, n_0)$  reaction involves the excitation and emission of the  $d_{5/2}$  valence neutron, analogous to the neutron pick-up reaction. Comparison of the  $^{17}\text{O}(\gamma, n)$  and  $^{17}\text{O}(\gamma, n_0)$  cross sections shows that the ground-state photoneutron reaction is concentrated just above threshold, in the pygmy resonance. As the pygmy resonance occurs at a low energy, it dominates the "bremsstrahlung-weighted" integrated cross section due to the shape of the bremsstrahlung spectrum: The "bremsstrahlung-weighted" integrated cross section for the  $^{17}\text{O}(\gamma, n_0)$  reaction is 30% of the "bremsstrahlung-weighted" cross section for the total  $^{17}\text{O}(\gamma, n)$  reaction, but only contributes 10% of the integrated cross section. It was therefore decided to subtract the measured<sup>10</sup>  $^{17}\text{O}(\gamma, n_0)$  cross section from the total photoneutron cross section<sup>1</sup> before calculating the relative population of the 6.13-MeV level. After this correction the results indicate that  $(3.9 \pm 0.8)\%$  of the "bremsstrahlung-weighted" cross section of the  $^{17}\text{O}$  GDR goes to the 6.13-MeV ( $3^-$ ) level in  $^{16}\text{O}$ . From the neutron pick-up

reaction  $^{17}\text{O}(d, ^3\text{H})^{16}\text{O}$  (Ref. 16) this level has a spectroscopic factor of 0.46. The comparison between the spectroscopic factors and the relative population of states in  $^{16}\text{O}$  are shown in Table IV, along with the wave functions of the states of interest. As the same states are populated in the photoneutron reaction and the neutron pick-up reaction, we conclude that the photoneutron reaction proceeds via a semidirect reaction mechanism.

The work of Jury *et al.*<sup>1,10</sup> shows that the  $^{16}\text{O}$  ground state is also strongly populated; significantly, this level has a spectroscopic factor of 0.74. Although no observations could be made about the population of unbound levels in  $^{16}\text{O}$ , this work suggests that there is a significant population of these levels. These levels have a summed  $C^2S$  of 4.53 from the work of Mairle *et al.*<sup>16</sup>

## V. SUMMARY

In conclusion, the results of this experiment indicate that the  $^{17}\text{O}(\gamma, p)^{16}\text{N}$  reaction is dominated by a semidirect reaction mechanism, with approximately 10% of the reaction being via decay from the preequilibrium stage or compound nucleus. The  $^{17}\text{O}(\gamma, n)^{16}\text{O}$  reaction is also dominated by a semidirect reaction mechanism, populating the  $^{16}\text{O}$  ground state and 6.13-MeV ( $3^-$ ) level only. No evidence of decay from the preequilibrium stage or compound nucleus is observed.

## ACKNOWLEDGMENTS

One of the authors (G.V.O'R.) acknowledges the support of a Commonwealth Post-Graduate Research Award, and another (D.Z.) the support of a University of Melbourne Research Award. We would also like to thank the Lawrence Livermore Research Laboratory for the loan of the  $^{17}\text{O}$ -enriched water sample.

\*Present address: Physics Department, The George Washington University, Washington, D.C., 20052.

<sup>1</sup>J. W. Jury, B. L. Berman, D. D. Faul, P. Meyer, and J. G. Woodworth, *Phys. Rev. C* **21**, 503 (1980).

<sup>2</sup>D. Zubanov, M. N. Thompson, B. L. Berman, R. E. Pywell, J. W. Jury, and K. G. McNeill, in *Proceedings of the 10th AINSE Conference on Nuclear Physics* (Australian Institute of Nuclear Science and Engineering, Canberra, 1984), Paper 63; University of Melbourne Report UM-P-89/43, 1989.

<sup>3</sup>J. S. Pruitt and S. R. Domen, *Natl. Bur. Stand. Monograph* No. 48 (U.S. GPO, Washington, D.C., 1962).

<sup>4</sup>U. E. P. Berg, H. Wolf, B. Schafer, and K. Wienhard, *Nucl. Instrum. Methods* **129**, 155 (1975).

<sup>5</sup>J. E. M. Thomson and M. N. Thompson, *Nucl. Phys.* **A285**, 84 (1977).

<sup>6</sup>J. E. M. Thomson, Ph.D. thesis, University of Melbourne, 1976.

<sup>7</sup>F. Ajzenberg-Selove, *Nucl. Phys.* **A460**, 1 (1986).

<sup>8</sup>P. J. P. Ryan, Ph.D. thesis, University of Melbourne, 1980.

<sup>9</sup>L. I. Schiff, *Phys. Rev.* **83**, 252 (1951).

<sup>10</sup>J. W. Jury, J. D. Watson, D. Rowley, T. W. Phillips, and J. G. Woodworth, *Phys. Rev. C* **32**, 1817 (1985).

<sup>11</sup>J. E. M. Thomson, M. N. Thompson, and R. J. Stewart, *Nucl. Phys.* **A290**, 14 (1977).

<sup>12</sup>P. J. P. Ryan, M. N. Thompson, K. Shoda, and T. Tanaka, *Nucl. Phys.* **A371**, 318 (1981).

<sup>13</sup>R. A. Eramzhyan, B. S. Ishkhanov, I. M. Kapitonov, and V. G. Neudatchin, *Phys. Rev. Lett.* **136**, 229 (1986).

<sup>14</sup>J. P. Elliott and B. H. Flowers, *Proc. R. Soc.* **A242**, 57 (1957).

<sup>15</sup>G. E. Brown and A. M. Green, *Nucl. Phys.* **A75**, 401 (1966).

<sup>16</sup>G. Mairle, G. J. Wagner, P. Doll, K. T. Knopfle, and H. Breuer, *Nucl. Phys.* **A299**, 39 (1978).

<sup>17</sup>P. J. P. Ryan and M. N. Thompson, *Nucl. Phys.* **A457**, 1 (1986).

<sup>18</sup>R. A. Sutton, M. N. Thompson, M. Hirooka, T. Tanaka, and K. Shoda, *Nucl. Phys.* **A452**, 41 (1986).

<sup>19</sup>P. J. P. Ryan, M. N. Thompson, K. Shoda, and T. Tanaka, *Nucl. Phys.* **A411**, 105 (1983).

<sup>20</sup>A. P. Zuker, B. Buck, and J. B. McGrory, *Phys. Rev. Lett.* **21**, 39 (1968).